The Spatial Distribution of [O I] in Comet Hale-Bopp from 2,000 to 1×10^6 km: Evidence for Spatial Asymmetry

J. P. Morgenthaler, W. Harris, C. M. Anderson, F. L. Roesler,
F. Scherb, (University of Wisconsin),
R. J. Oliversen (GSFC), N. E. Doane (Raytheon ITSS),
W. H. Smyth (AER), and M. L. Marconi (FPRI)

May 31, 1999

Abstract

The exceptional brightness and long observational window of comet Hale-Bopp provided a remarkable opportunity to study both the neutral coma and the plasma in the coma and ion tail. Our team of observers from UW–Madison and Goddard Space Fight Center used seven different instruments at Kitt Peak to observe cometary emission from H, OH, O, H_2O^+, NH_2, C, CN, C_2, and the continuum. Here we present observations and model analysis for the $O(^1D)$ ([O I] 6300 Å) emission. The data were taken by three telescopes on Kitt Peak: the Wisconsin, Indiana, Yale NRAO (WIYN), Wisconsin H-α Mapper (WHAM), and the NSO McMath-Pierce. The 3.5-meter WIYN telescope recorded up to 96 simultaneous spectra with a Multi-Object Spectrograph (MOS), the WHAM Fabry-Perot spectrometer recorded spectra and narrow-band images over a 1° field of view and the 2-inch Fabry-Perot spectrometer at the McMath-Pierce main telescope recorded high resolution ($\lambda/\Delta\lambda$ = 80,000) spectra of the [O I] 6300 Å emission with a 6 arcminute field of view. The combination of MOS and Fabry-Perot data covers spatial scales ranging from 2,000 km to 1×10^6 km. The data consistently show a tailward asymmetry in the [O I] emission. Previous comets have shown spherically symmetric [O I] emission which has been well described by the Monte Carlo Particle Trajectory Model (MCPTM) of Combi & Smyth (1988) with recent refinements by (Combi, Bos, & Smyth 1993) for an oxygen source produced by photodissociation of H_2O from the nucleus. We use this model to fit regions of the [O I] distribution away from the tailward enhancements and find that the excess emission in the tailward direction is ∼30 Rayleighs at 500,000 km from the nucleus for late February to mid March. We discuss several possible mechanisms for creating this emission asymmetry.

Table 1: Preliminary H_2O Branching Ratios for conditions near solar minimum (from Smyth *et al.* 1993).

Reaction	Branching Ratio
$H_2O + h\nu \rightarrow H_2 + O(^1D)$	BR1 = 0.034
$H_2O + h\nu \rightarrow H + OH$	BR2 = 0.876
$OH + h\nu \rightarrow H + O(^1D)$	BR3=0.049–0.059

Introduction

Water is the most abundant volatile species in the comae of comets. Water is photo-dissociated by sunlight according to the reactions listed in Table 1. The $O(^1D)$ state is indicated schematically in Figure 1.

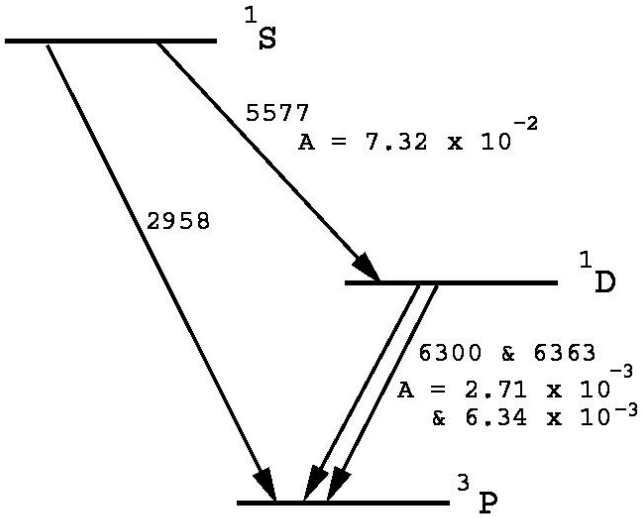

Figure 1: Portion of atomic oxygen energy level diagram. Einstein A values are in units of s^{-1}.

The decay of $O(^1D)$ is easily detected with spectroscopic techniques or narrow-band imaging. In this work, we measure the 6300 Ådecay path, often denoted [O I]6300, or in this paper, sim-

ply [O I]. We can arrive *directly* at the comet water production rate, $Q(H_2O)$ with the following equations:

$$Q(O(^1D)) = \left(\frac{4}{3}\right)(4\pi\Delta^2\Omega I_{6300})AC \quad (1)$$

$$Q(H_2O) = \frac{Q(O(^1D))}{BR1 + (BR2)(BR3)} \quad (2)$$

where the factor of $4/3$ corrects for the emission we do not measure in the 6364Å decay path of $O(^1D)$, Δ is the distance between the earth and the comet, Ω is the solid angle of the field of view, I_{6300} is the average 6300 Å surface brightness over the field of view in photons s^{-1} cm^{-2} sr^{-1}, AC is the aperture correction, which corrects for the emission outside our field of view, and preliminary values of the branching ratios, BRn are given in Table 1.

We have used the state-of-the-art Monte Carlo Particle Trajectory Model (MCPTM) of Combi & Smyth (1988) including recent refinements (Combi, Bos, & Smyth 1993) to describe the *distribution* of water and its photo-dissociation products for projected distances between 10,000 and 1×10^6 km from the comet nucleus. Since solar radiation tends to dissociate water molecules rather than impart momentum and the solar wind has a small cross-section of interaction with water, the distribution of water, and hence $O(^1D)$, is expected (and generally observed) to be spherically symmetric (e.g. Halley: Magee-Sauer *et al.* 1988, Austin: Schultz *et al.* 1993). Here we produce conclusive evidence of an asymmetry in the [O I] distribution and discuss some possible mechanisms for its cause.

Observations

Observations of comet Hale-Bopp over a wide range of wavelengths were conducted by this team from Aug 16, 1996 through April 29, 1997. This poster presents [O I] observations from February to April 1997, which were recorded by four instruments on Kitt Peak.

On 6 nights the Hydra positioner of the 3.5-meter Wisconsin, Indiana, Yale, NRAO (WIYN) Telescope Multi Object Spectrograph (MOS) was used to place up to 96 fibers in concentric rings around the nucleus to as much as 22.5 arc minutes in radius (see Figure 2). The MOS spectra were recorded over a 300 Å range centered at 6250 Å with a resolving power of $(\lambda/\Delta\lambda)$ ~15,000. On 4 nights a 7 by 13 array of 3 arc second fibers on 4 arc second centers known as Densepak was used on the WIYN MOS to probe the inner coma.

On three nights, the 6-inch Fabry-Perot spectrometer that comprises the Wisconsin H-α Mapper (WHAM), recorded narrow band images over a 1° field of view. WHAM can record spectra over a 200 km/s range (4 Å at 6300 Å) with a resolving power of $(\lambda/\Delta\lambda)$ ~30,000, or narrow band images over as little as ~10 km/s.

On 29 nights a 2-inch Fabry-Perot spectrometer on the NSO McMath-Pierce main telescope recorded high resolution ($\lambda/\Delta\lambda$ = 80,000) spectra of the [O I] 6300 Å emission with a 6 arcminute field of view.

The combination of MOS and Fabry-Perot data covers spatial scales ranging from 2,000 km to 1×10^6 km.

Results

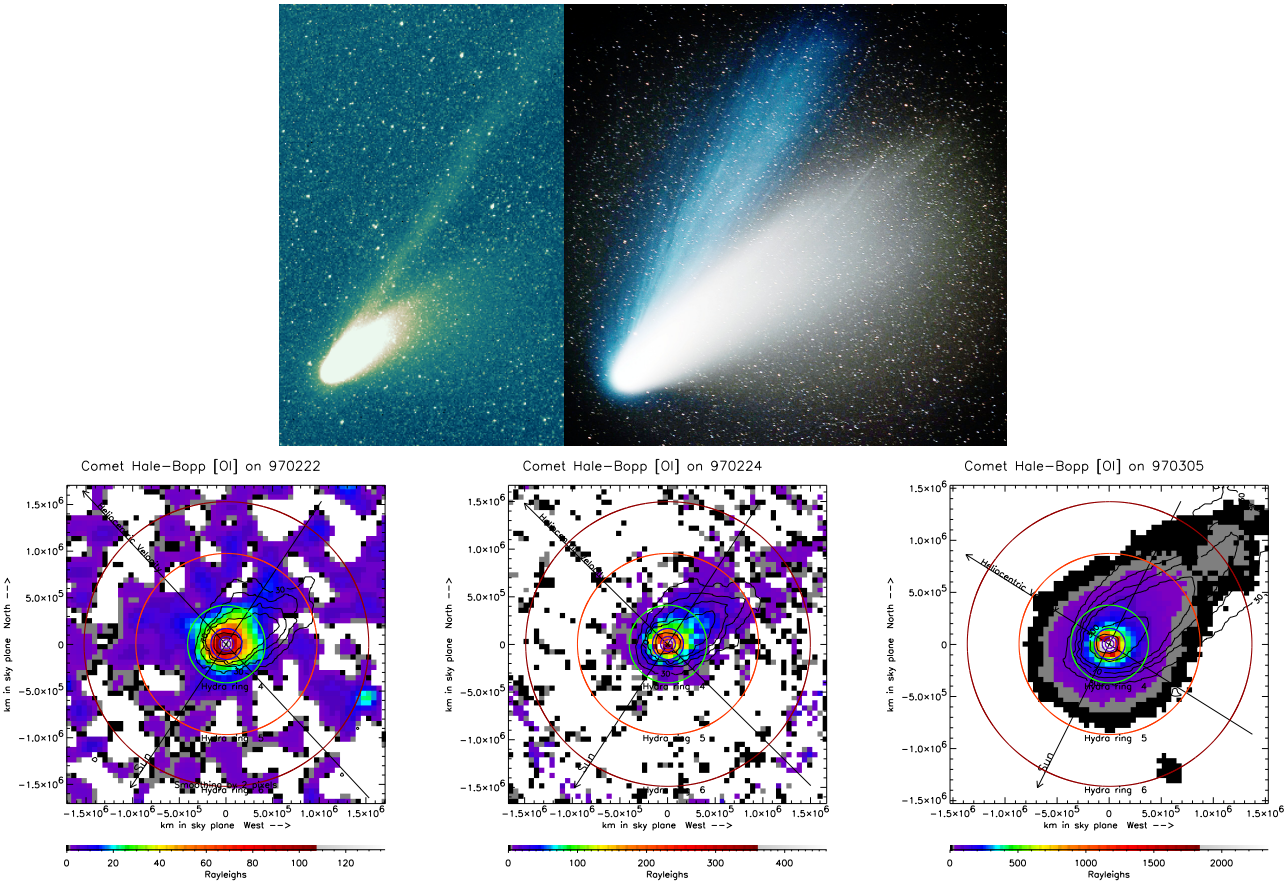

Figure 2: Hale-Bopp images with [O I] emission is shown in color, dust in contours, and circles showing positions of annuli used for comparison to Hydra data in Figure 3. The WHAM field of view is 1° in diameter. Inset images courtesy of H. Mikuz & B. Kambic (http://www.amtsgym-sdbg.dk/as): false color H_2O+ image showing ion tail on 1997 March 5 (top) and color photograph from 1997 March 9 (bottom). These images cover 5-10 degrees.

Figure 2 shows three WHAM [O I] images, the ion tail, and a color photo of the comet. The Feb 22 [O I] image has been smoothed to reduce noise. Since the WHAM field of view is so large, we can use equations 1 and 2 with the aperture correction

$AC = 1$ to arrive directly at a water production rate. These rates are summarized in Table 2.

Table 2: Water production rates from WHAM data, preliminary results.

UT date (1997)	$R_{\rm helio}$ (AU)	Q($O(^1D)$) (s^{-1})	Q(H_2O) (s^{-1})
Feb 22	1.12873	7.1×10^{29}	9×10^{30}
Feb 24	1.10936	8.4×10^{29}	1×10^{31}
Mar 5	1.02930	4.3×10^{30}	6×10^{31}

Figure 3 plots the measured Hydra [O I] surface brightness versus position angle. We present the WHAM data in a similar format for comparison purposes. On Feb 24, Mar 2, and Mar 16, the [O I] asymmetry appears to be associated with the dust tail. On Mar 5, the brightest [O I] emission in ring 4 is very close to the ion tail, but the ring 5 [O I] emission follow the dust more closely.

Figure 4 shows the radial profiles of all of the datasets that have been reduced so far. For the WHAM data, the radial profile of the quadrants centered on the anti-sunward direction are plotted separately. The Feb 24 and Mar 5 data show pronounced asymmetry.

Many of our high-resolution 2-inch Fabry-Perot spectra show an asymmetric $O(^1D)$ velocity distribution (Figure 5). The red tails on these spectra are consistent with material flowing in the anti-sunward direction at 5-10 km/s.

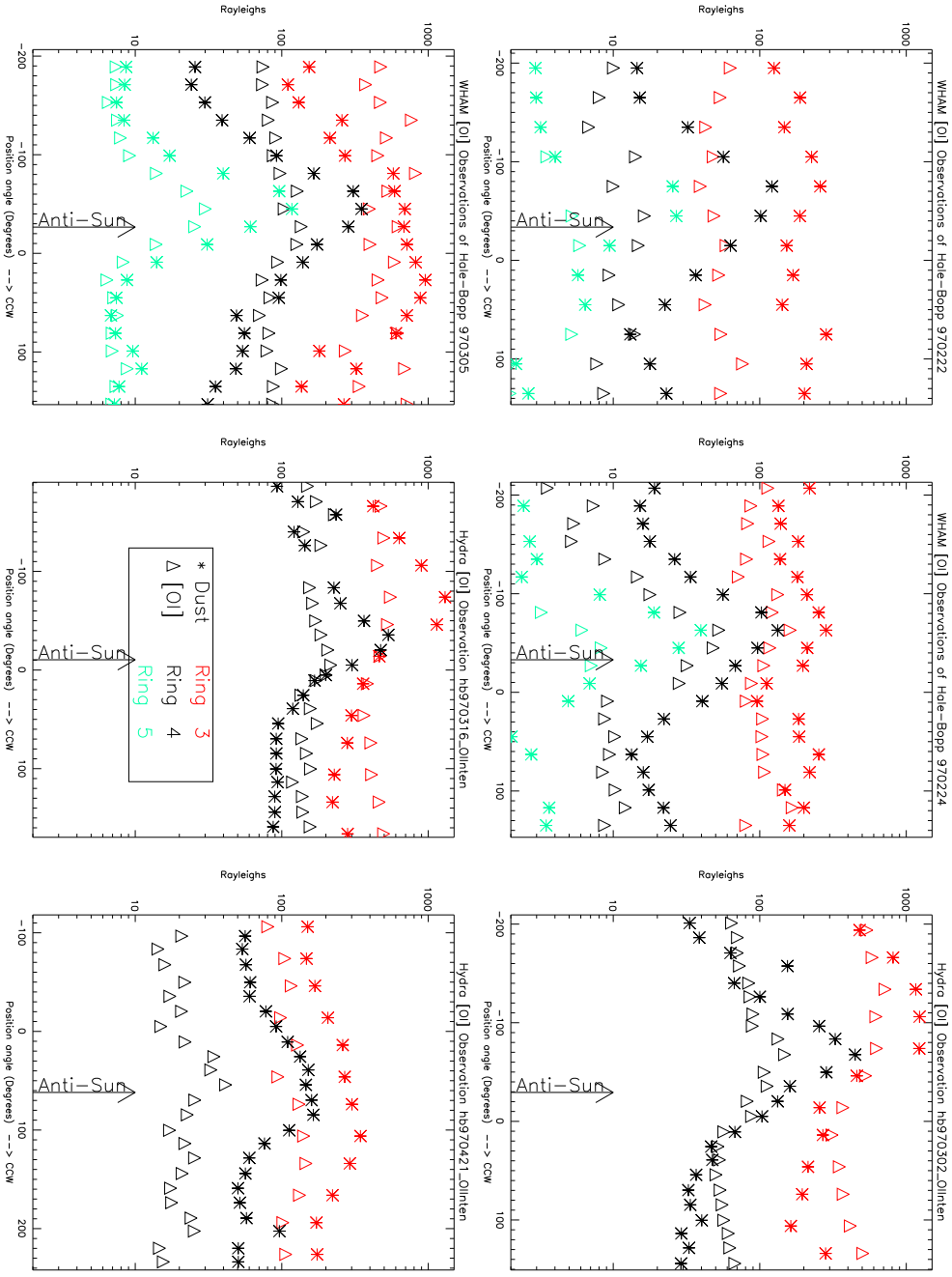

Figure 3: Comparison of WHAM and Hydra [O I] data. Focus on the black triangles, which indicate the [O I] surface brightness at a radius of 6 arcminutes ($\sim$ 360,000 km).

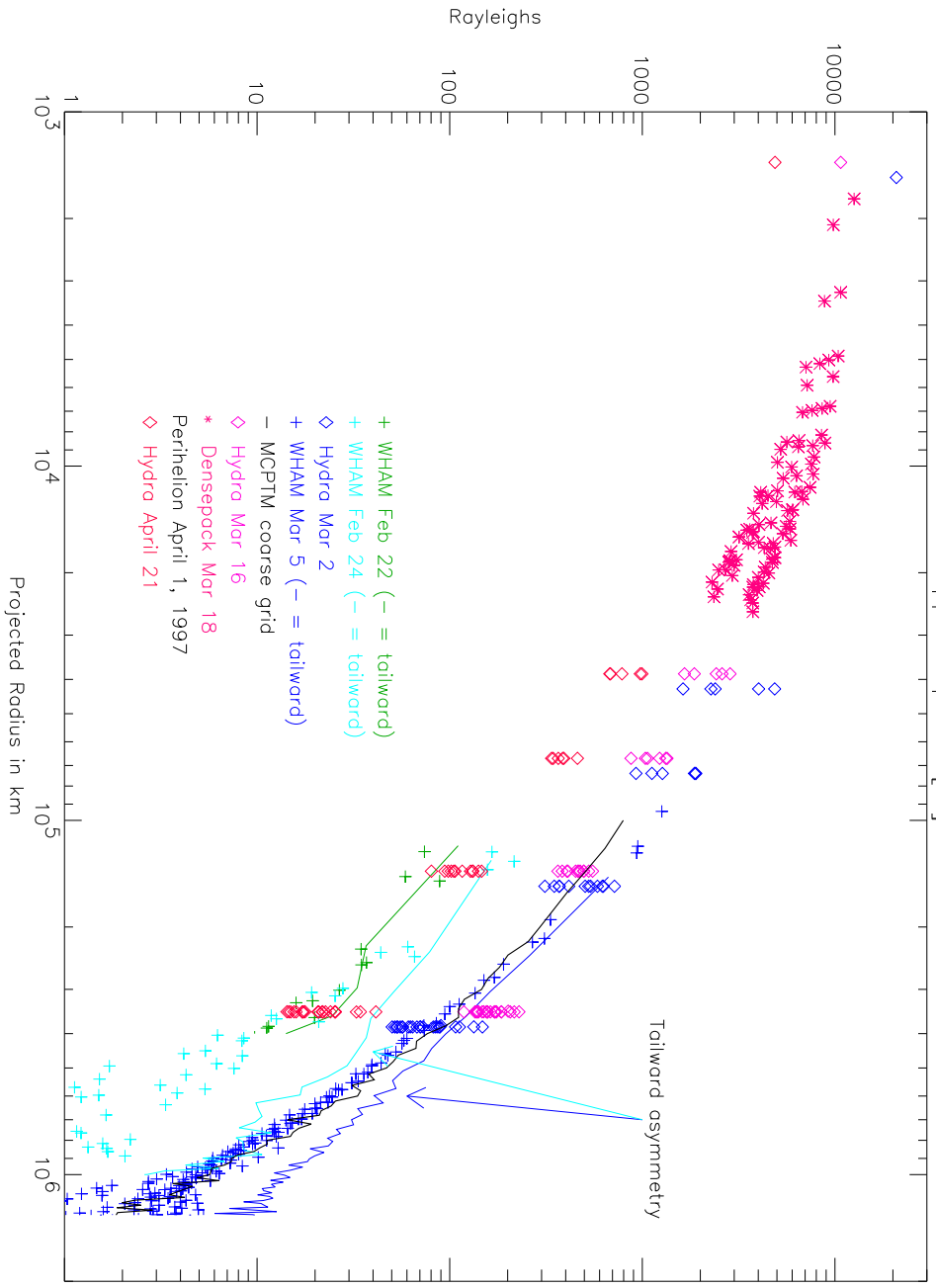

Figure 4: Radial profiles of [O I] emission in comet Hale-Bopp. The Densepak and Hydra absolute calibration is good to better than 20%. The WHAM absolute calibration is not complete yet.

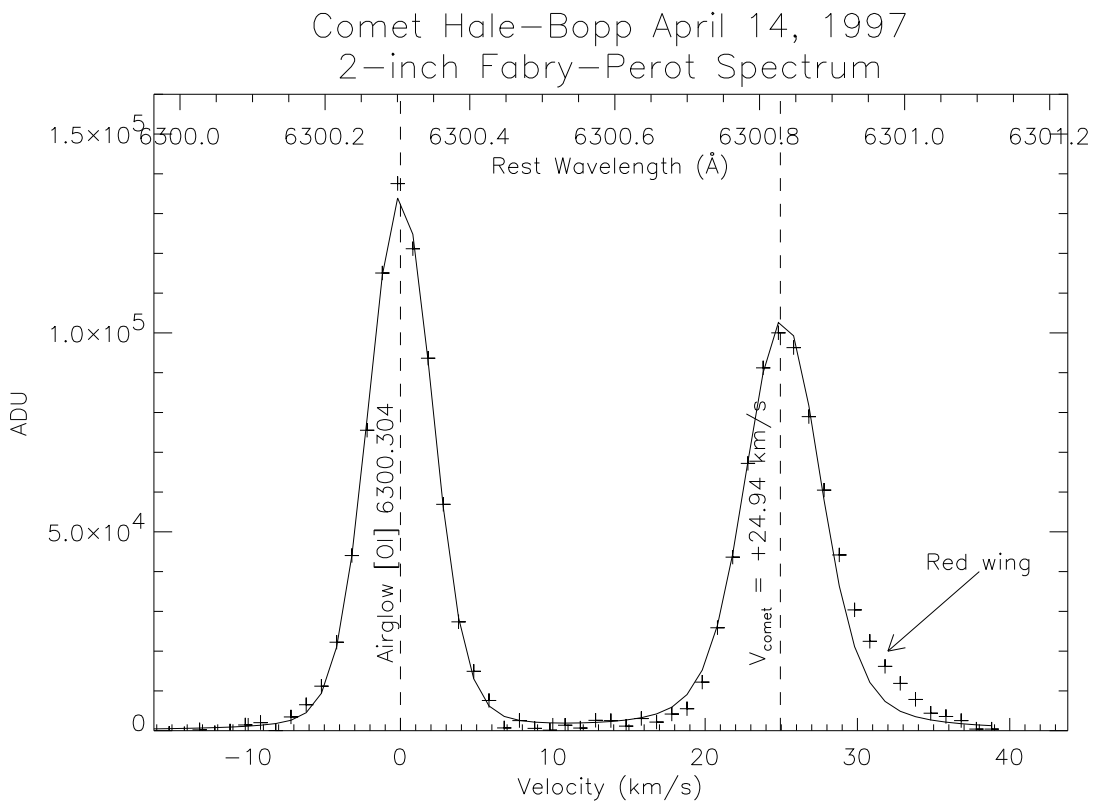

Figure 5: 2 inch Fabry-Perot spectrum of comet Hale-Bopp on April 14, 1997. The field of view is 200,000 km in radius, centered on the comet head. The red tail on the velocity distribution is consistent with material flowing tailward.

The fact that three very different observing techniques show asymmetry for observations covering a 2 month time span around perihelion is strong evidence that the [O I] asymmetry is a detectable and lasting effect.

What causes the Tailward Asymmetry?

Briefly: we do not know yet! Table 3 lists some of the mechanisms we are considering together with some preliminary estimates of the [O I]6300 surface brightness of each effect. The tailward flow of O(^{1}D) implied by Figure 5 and the correlation of the peak in the [O I] asymmetry with the ion tail in ring 4 of the March 5 WHAM image is circumstantial evidence that

suggest the ion tail is the primarily responsible

Table 3: Possible Causes of [O I]6300 asymmetry. Observed asymmetric excess is ∼30 R.

Mechanism	f_γ (see text)	*Rough* Value (Rayleighs)
Dust scattering O(^{1}D) from nucleus	-	4×10^{-9}
Excitation of O to O(^{1}D) by solar wind	0.99	0.2
Excitation of O to O(^{1}D) by ion tail electrons	0.99	12
Dissociation of OH by ion tail electrons		
Dissociation of H_2O by ion tail electrons		
Dissociation of H_2O+ by ion tail electrons	10^{-3}	0.5
Dissociation of CO by ion tail electrons		
Dissociation of CO_2 by ion tail electrons		
Dissociation of CO+ by ion tail electrons	< 0.2	< 6
Dissociation of CO_2+ by ion tail electrons	< 0.2	< 14
Distributed asymmetric source of water		
Transient source		
Distributed asymmetric source of CO		
H_2O^+ dissociative recombination		
CO^+ dissociative recombination		
CO_2^+ dissociative recombination		

We calculate the contribution from dust in the tail scattering [O I]6300 produced in the nuclear region by using the [O I] and continuum WHAM images and the solar irradiance in the

WHAM bandpass ($\sim 10^{13}$ phot cm^{-2} s^{-1}).

To calculate the surface brightness, σ, of [O I] produced by electron impact on species γ, where γ can be water, oxygen, OH, O, CO, etc., we use the expression:

$$\sigma = \frac{N_\gamma n_e r}{4\pi} \tag{3}$$

where r is the rate coefficient in cm^3 s^{-1}, N_γ is the column density of species γ and n_e the number density of electrons along the line of sight. Given a water production rate of n ($\sim 10^{31}$ s^{-1}), the density of species γ at a distance r from the nucleus can be approximated:

$$\rho_\gamma(r) = \frac{nf}{4\pi r^2 v} \tag{4}$$

where f is the number of species γ atoms/molecules per water molecule and v is the outflow velocity (2 km/s). Integrating this quantity over the portion of the ion tail along the line of sight at a projected distance of b from the nucleus, we arrive at an approximate expression for the surface brightness, σ, of [O I] produced by electron impact on species γ:

$$\sigma_\gamma = \frac{0.09 n f_\gamma n_e r_\gamma}{(4\pi)^2 bv}. \tag{5}$$

The factor of 0.09 comes from a rough approximation of the tail geometry in early March.

Conclusion

In addition to providing data for determining water production rates, our O(^{1}D) measurements show a tailward extension which has not been observed in other comets. Preliminary calculations indicate that production of O(^{1}D) by electrons in the ion tail is a possible source of this asymmetry, though much of the data suggests that emission is more closely associated with the dust tail.

The authors would like to thank Mike Combi for providing the results of his electron density calculations before publication.

References

Combi, M. R., Bos, B., & Smyth, W. 1993, ApJ, 408, 668

Combi, M. R., & Smyth, W. H. 1988, ApJ, 327, 1026

Magee-Sauer, K., Roesler, F., Scherb, F., Harlander, J., & Oliversen, R. 1988, Icarus, 76, 89

Scherb, F. 1981, ApJ, 243, 644

Schultz, D., Li, G. S. H., Scherb, F., & Roesler, F. 1993, Icarus, 101, 95

Smyth, W. H., Marconi, M. L., Scherb, F., & Roesler, F. 1993, ApJ, 413, 756